Polymer Journal, Vol. 33, No. 2, pp 139—146 (2001)

Effect of Thermal History on the Phase Behavior of *N*-Methyl Morpholine *N*-Oxide Hydrates and Their Solutions of Cellulose

Dong Bok KIM, Wha Seop LEE,* Seong Mu JO,* Young Moo LEE, and Byoung Chul KIM

Division of Chemical Engineering, Hanyang University, Haingdang, Seongdong, Seoul 133-791, Korea
**Polymer Hybrid Center, Korea Institute of Science and Technology, Seoul 136-791, Korea*

(Received July 19, 2000; Accepted November 13, 2000)

ABSTRACT: *N*-Methyl morpholine *N*-oxide (NMMO) hydrates, used in the preparation of cellulose spinning dope for lyocell manufacturing, have various crystal structures according to the hydration number (n). A single melting peak for solid-solid transition from NMMO monohydrate to anhydrous NMMO at 94℃ was previously reported. However, we observed the melting peak at 90℃ ascribed to the solid-solid transition from NMMO monohydrate to anhydrous NMMO and another melting peak observed in the range from 98 to 105℃ when $n<1$. This discrepancy resulted from the experimental errors in differential scanning calorimetry (DSC) measurement. The pressure capsule enabled us to obtain precise and reproducible DSC data of NMMO hydrates. The three different crystal structures of NMMO hydrates with $n<1$ were identified by crystallization experiments. The crystal, which had melted in the range from 90 to 105℃ during heating (shown by double peaks), was recrystallized at 80℃ during cooling, which has never been reported. The NMMO hydrates with $n<1$ required heating above 130℃ to produce a homogeneous melt, and the required temperature was increased up to 180℃ for anhydrous NMMO. If the heating temperature was not high enough to fully melt the NMMO hydrate crystal, the unmelted NMMO hydrate crystals affected the thermal responses of the hydrate and its phase behavior of cellulose solutions in the NMMO hydrate.

KEY WORDS Phase Behavior / *N*-Methyl Morpholine *N*-Oxide Hydrate / Cellulose / *N*-Methyl Morpholine *N*-Oxide Hydrate Solution / Solid-Solid Transition /

Recently the *N*-methyl morpholine *N*-oxide (NMMO) hydrates attract much attention of cellulose processors because it is a versatile solvent of cellulose in the commercial production of lyocell fibers and cellulose films by direct dissolution method.[1-9] They dissolve cellulose through hydrogen bonding by the N–O group of NMMO. Anhydrous NMMO best dissolves cellulose but unfavorable as the solvent because of high melting temperature (T_m) 172℃, which readily causes the thermal degradation. The T_m and solvating power of NMMO hydrate are dependent on the value of n.[10-13] Commercial lyocell spinning generally adopts solutions of cellulose in NMMO hydrates with n, range from 0 to 1.0.

The value of n of NMMO hydrates has a significant influence on the phase behavior of the cellulose solutions.[9,14] The NMMO hydrates with $n=1$—1.5 are reported to produce isotropic cellulose solutions and anisotropic solutions are recognized to be obtained by using the NMMO hydrates with $n<1$. Up to now, however, the reason for the phase behavior of the cellulose solutions with the value of n is not clear although some rheological attempts were made to account for the phenomenon.[15-17]

It is prerequisite to characterize the thermal properties of NMMO hydrates to obtain a precise phase diagram of the cellulose solutions with the value of n. Lots of thermal analyses on the NMMO hydrates have been carried out to understand the phase behavior of the solution.[8,9,18-23] A careful examination of their experimental conditions raises questions about the reproducibility of results. They prepared NMMO hydrates with $n\leq 1$ by heating the simple mixture of anhydrous NMMO and water[9] although it is necessitated to obtain homogeneous NMMO hydrates to heat the mixture above the T_m of anhydrous NMMO, 180℃. If heated below the T_m NMMO crystals still remain embedded in the NMMO hydrate matrix even after the fusion process. The unmelted crystals surely affect the phase behavior of the cellulose solution in the NMMO hydrates as well.

The NMMO hydrates with different values of n are reported to exhibit different crystallization behaviors and produce different crystal structures. In the phase transition of cellulose solutions the crystallization behavior of the NMMO hydrates themselves would be included when their phase transition temperature folds on the transition temperature of the cellulose solutions. This frequently draws erroneous conclusions on the phase behavior of the cellulose solutions. To clear out this uncertainty, the crystal structure and thermal behavior of NMMO hydrates themselves were discussed in relation with the phase behavior of cellulose solutions in the hydrates.

EXPERIMENTAL

Materials and Sample Preparation

NMMO/H_2O (50 wt%/50 wt%) was purchased from Aldrich Co. The aqueous NMMO solution was condensed step by step in a rotary evaporator in the range from 60 to 100℃ for 3 h at the reduced pressure to produce the NMMO hydrate melts with desired hydration level. They were solidified and powdered in the glove box in nitrogen atmosphere. The cellulose sample, Rayonex-P, was supplied by ITT Rayonier Co., whose weight-

average degree of polymerization (DP_w) was 600. It was dried at 80℃ for 24 h prior to use.

The moisture-free cellulose was dissolved in a NMMO hydrate at the concentration of 6, 10, 12, 15, 18, and 20 wt%. The homogeneous cellulose solutions were prepared by dissolving and defoaming the powdered granules for 40 min. at 120℃ for $n=1$ and at 140℃ for $n=0.65$. To minimize the experimental errors originating from the thermal decomposition of cellulose, an antioxidant, *n*-propyl gallate (0.5 wt% for cellulose), was introduced to the solution.

Measurement of Physical Properties

The amount of hydrated water was determined by the method suggested by Fischer.[24] The measured water content in the NMMO hydrates, from 3 to 22 wt%, corresponded to the values of n, from 0.23 to 1.65. The thermal properties of NMMO hydrates and cellulose solutions in the hydrates were measured by Perkin–Elmer DSC 7 in nitrogen atmosphere. In differencial scanning calorimetry (DSC) measurement the stainless steel crucible (Perkin–Elmer part 319-0218) was used, which was equipped with an O-ring to withstand the high pressure generated by steaming of water. For comparison DSC measurement without an O-ring was also performed. The scan rate was 2, 5, and 10℃ min^{-1}. The cooling experiments were carried out after having heated the condensed NMMO hydrates to different temperatures, in the range from 90 to 160℃, corresponding to the value of n, from 1.0 to 0.45. In the case of the NMMO monohydrate, the cooling thermograms were obtained after heating up to the temperatures range from 90 to 120℃. The NMMO monohydrate whose T_m was 78℃ was placed in the crucible and heated up to 90℃, and the sample was loaded in DSC for 30 s at this temperature, then cooled. The same procedure was repeated for the sample three times but the ultimate heating temperature was changed; 100 for the second scan, 110 for the third scan, and 120℃ for the fourth scan. The same experiment was carried out for the NMMO hydrates with n, from 0.9 to 0.45 by heating the hydrates up to the range from 90 to 160℃.

RESULTS AND DISCUSSION

Thermal Transition of NMMO Hydrates

Homogeneous NMMO hydrate melts could be prepared by evaporating the excess water from a dilute aqueous NMMO solution. The DSC thermograms of thus prepared NMMO hydrates are shown in Figure 1. Different (T_m)s have been reported for the NMMO monohydrate by different researchers; 72,[8] 75,[11] and 78℃.[10] Our result was 78℃ at the scan rate 5℃ min^{-1}. The NMMO hydrates gave an identical melting peak in the first and second heating scans when an O-ring crucible pan was employed in DSC measurement. This indicates that little thermal decomposition takes place during dissolution and DSC measurement. In the case of anhydrous NMMO, however, the thermal decomposition was inevitable during melting in the absence of an antioxidant. Hence, it gave different melting peaks during the first and second scans.

The remaining unmelted NMMO hydrate affected the crystallization behavior of NMMO hydrate as shown in Figure 1. The NMMO hydrate with $n=0.9$ shows different thermal behaviors with the NMMO monohydrate when heated up to the range from 90 to 130℃. The NMMO hydrate gives a single melting peak at 78℃, and the endothermic peak in the range from 90 to 100℃ is slightly increased. The extent of the increase of the endothermic peak is increased with decreasing the value of n (compare $n=0.65$ with $n=0.45$). In addition, the NMMO monohydrate shows only one crystallization peak in the range from 20 to 30℃ on the cooling scan, which corresponds the melting of the NMMO monohydrate crystals at 78℃. However, the NMMO hydrate with $n=0.9$ shows 2 crystallization peaks, and the NMMO hydrates with $n=0.65$ and 0.45 give 3 crystallization peaks. When the maximum heating temperature of the NMMO hydrate samples reaches 120 ($n=0.9$), 110 ($n=0.65$), and 100℃ ($n=0.45$), the secondary crystallization takes place in the range from 70 to 80℃. It is well characterized from the definite heat of crystallization that the weak melting peaks in the range from 90 to 100℃ stands for the correspondent crystal structures. The NMMO monohydrate melts first, and succesive melting of remaining crystals of NMMO hydrates follows. This gives very small sensible heat of fusion of the DSC crucible pan, giving rise to very weak peak intensity.

When the maximum heating temperature is raised to 110 ($n=0.9$), 130 ($n=0.65$), and 150℃ ($n=0.45$), the cooling scan shows a shift of the crystallization peaks observed in the range from 20 to 30℃ to a higher temperature. This is obliged to the fact that the crystallized NMMO hydrates with $n<1$ play the role of a nucleating agent in the crystallization of NMMO monohydrate. In fact, if we raise the maximum heating temperature up to the critical temperature the T_c converges to a fixed value; for example, 140 for $n=0.65$ and 160℃ for $n=0.45$.

It should be also noted that the NMMO hydrate with $n=0.65$ exhibits a weak peak at 90℃ which has never been reported by others. This may be ascribed to the mixed crystals of NMMO hydrates. On this experimental basis it is recommended that a high temperature melting is essential in the preparation of a homogeneous cellulose solutions particular when NMMO hydrates with small hydration numbers; 130 for $n=0.9$ and 160℃ for $n=0.45$.

For the comparison purpose the melting behavior of the NMMO hydrates was examined by using ordinary DSC pan without O-ring and crucible DSC pan with O-ring, and the result shown in Figure 2. Figure 2a represents the thermal behavior of NMMO with $0.23<n<1.0$ measured by DSC crucible pan. In this case an equilibrium state exhibits a consistent thermogram of NMMO hydrate because the evaporation of steaming water is absolutely prevented. The NMMO hydrates with $n=1.0$ give a single melting peak at 78℃. When $n\leq0.83$ other melting peaks are observed over the temperature range from 90 to 178℃ in addition to 78℃, which is more prominent with the NMMO hydrates with smaller values of n, verifying the coexistence of various crystal structures.

On the other hand, Figure 2b shows the effect of

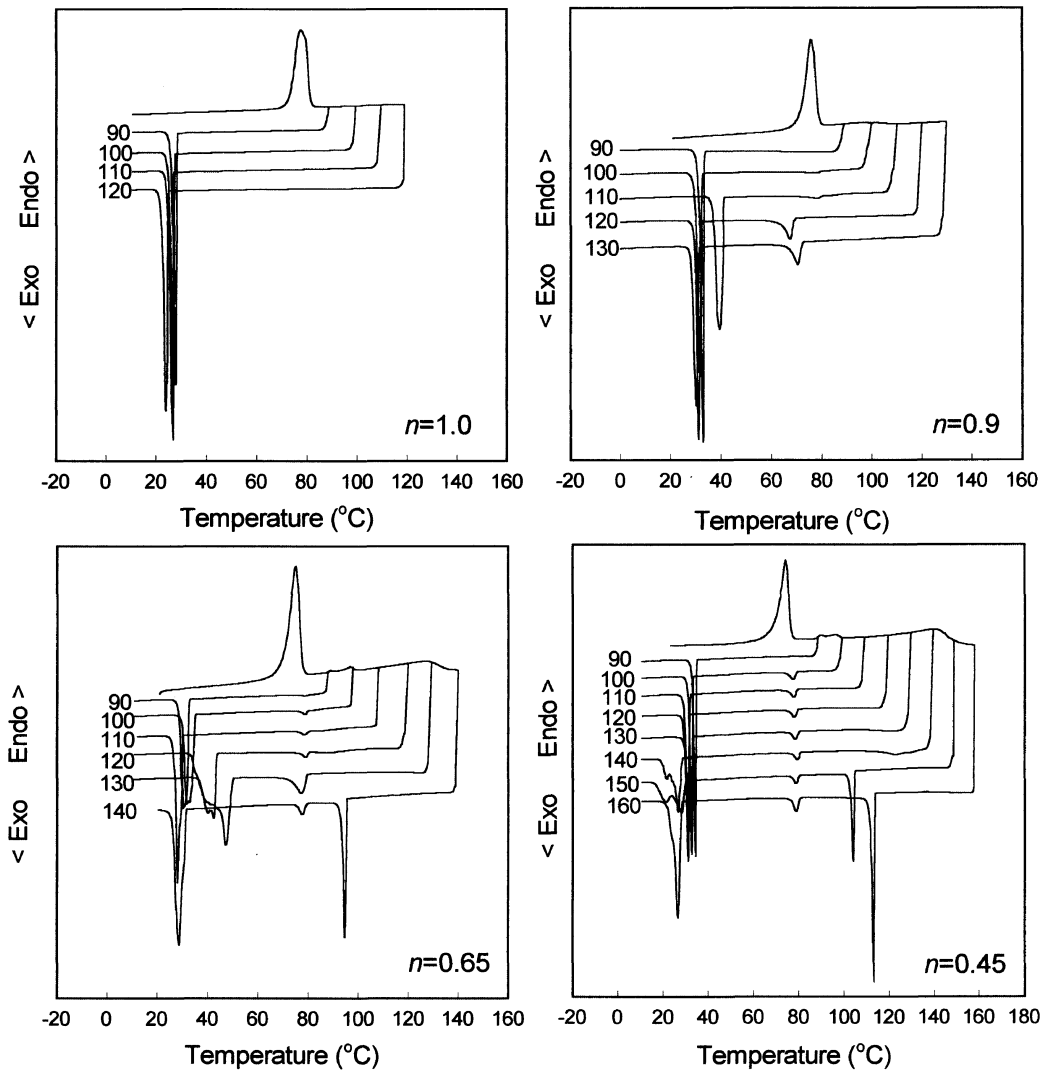

Figure 1. DSC cooling-scan thermogram of various NMMO hydrates at the scan rate 5℃ min^{-1}, showing the effect of the hydration number of NMMO hydrates and the ultimate melting temperature during heating scan on the cooling crystallization behavior of the hydrates.

Table I. Variation of melting and crystallization point of NMMO hydrates at scan rate of 5℃ min^{-1}

Hydration number	Ordinary DSC pan							DSC crucible pan (with an O-ring)						
	T_m/℃				T_c/℃			T_m/℃				T_c/℃		
$n=1$	78				32			78				25		
$n=0.83$	78	—	—	—	32	81	—	78	90	98	115	29	79	83
$n=0.65$	78	—	94	—	31	82	85	78	90	98	129	29	78	95
$n=0.45$	78	—	98	135	27	80	127	78	90	98	140	27	79	114
$n=0.23$	76	—	99	170	—	79	133	76	90	102	159	—	80	124

evaporation of steaming water during DSC measurement, which was measured by using ordinary DSC pan without O-ring. Referring to the thermogram of NMMO hydrates with $0.23<n<1.0$ during heating one can observe the solid–solid transition from NMMO monohydrate to anhydrous NMMO over the temperature range from 94 to 98℃.

The continuous increase of the secondary melting peak is the direct evidence of the evaporation of water from the specimen during DSC measurement. That is, evaporating water lowers the temperature of the specimen in the DSC pan on account of heat of evaporation. Hence the secondary melting peak was observed at the temperature higher than the true T_m 90℃. The greater increase of the peak temperature at the low hydration level more clearly explains this. The third T_m also increases with decreasing the hydration level for the same reason. Consequently it can be suggested that the increase of the peak temperatures with decreasing the value of n in the previous studies[10] did not result from the true thermal transition of the specimens but resulted from experimental errors associated with the vaporization of water. Table I further ascertains the experimental errors. In the case of NMMO monohydrate the T_m was independent of the evaporation of steaming water as predicted. In the case of other NMMO hydrates

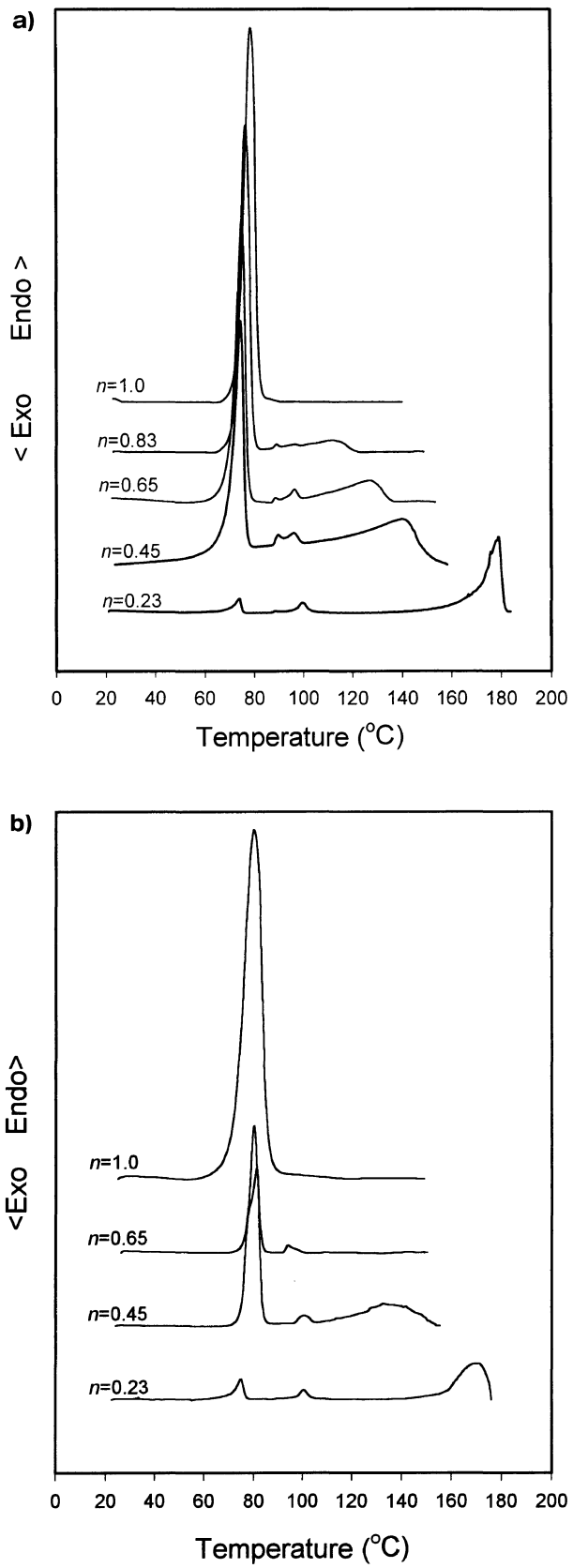

Figure 2. DSC thermograms of NMMO hydrates, showing the effect of hydration number in the NMMO hydrates: a) DSC crucible pan, b) ordinary DSC pan.

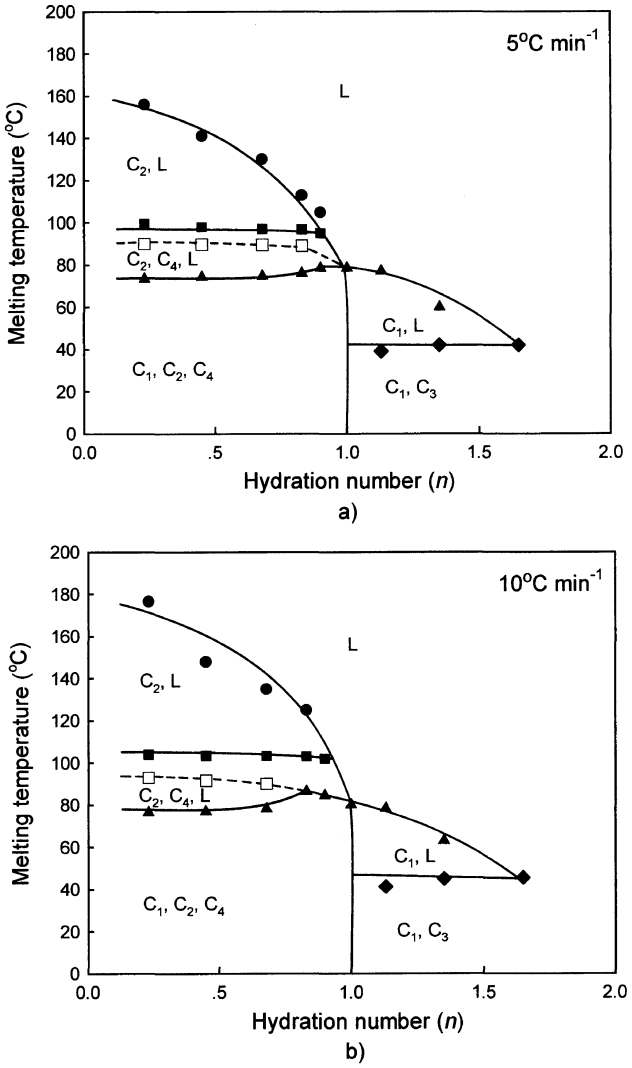

Figure 3. Relationship between melting temperature and hydration number in the NMMO hydrates system: a) 5℃ min^{-1} and b) 10℃ min^{-1}.

the evaporation of streaming water has a notable effect on the thermal transition of NMMO hydrates. Thus, the thermogram of the NMMO hydrates measured by the ordinary DSC pan without O-ring shows an increase of the melting peak from 94 to 98℃ with decreasing the value of n, which coincides exactly with the previous results by others.[10]

In addition, in the case of NMMO hydrate with $n = 0.23$, the T_m of the NMMO hydrates was observed at 170 and 159℃ when measured by ordinary DSC pan and DSC crucible pan with O-ring, respectively. This originates from the fact that the evaporation of steaming water reduces the value of n in the NMMO hydrates. For the same reason, the crystallization temperature shifts to higher temperature with the evaporation of steaming water.

Figure 3 plots the variation of the T_m of NMMO hydrates with hydration level. This type of plot for NMMO hydrates and cellulose solutions in NMMO hydrates has been widely used for its convenience.[10,25] This diagram assesses the variation of the T_m and the crystal structure of NMMO hydrates with value of n.[25] L represents liquid phase obtained by melting the crystals of C_1 (NMMO monohydrate), C_2 (anhydrous NMMO), C_3 (NMMO hydrate with $n = 2.5$), and C_4. C_4 reflects a solid –solid transition from NMMO monohydrate to anhy-

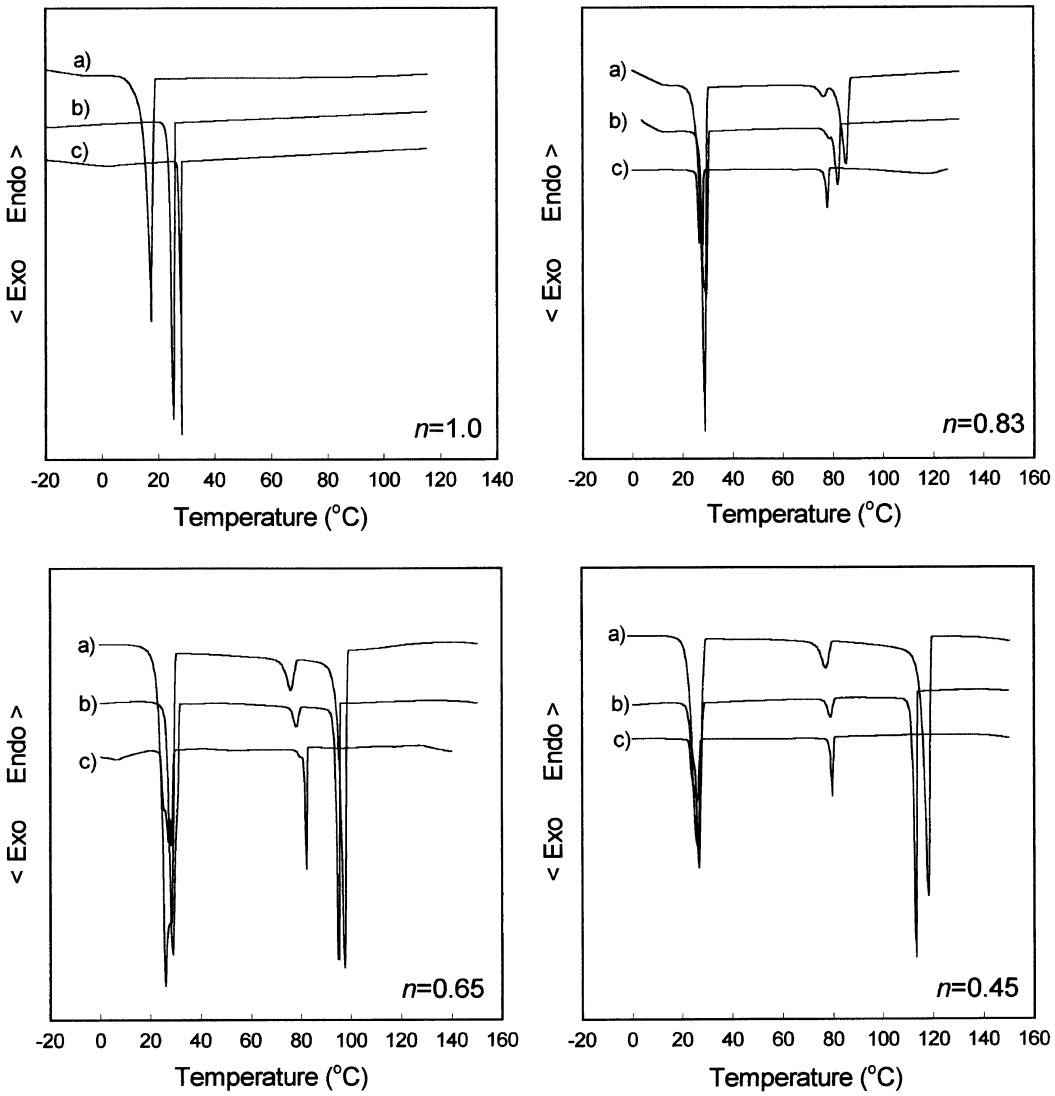

Figure 4. DSC thermograms of NMMO hydrates obtained during cooling at different cooling rates, showing the effect of hydration number and cooling rate: a) 10℃ min^{-1}, b) 5℃ min^{-1}, and c) 2℃ min^{-1}.

drous NMMO which was identified by the new peak at 90℃ (see Figure 2a). At $n=1.0$ the crystal of only C_1 exists, at $n<1$ the crystals of C_1, C_2, and C_4 coexist, and at $n>1$ the crystals of C_1 and C_3 coexist. At $n=2.5$ the crystal of only C_3 exists, whose melting point is 39℃. If the value of n ranges $0.9 \leq n < 1$ the crystals of C_1 and C_2 do not exhibit the melting peak at 90℃, which is attributable to the inhomogeneity of the NMMO hydrates. If $n \leq 0.83$ the melting peak at 90℃ is observed and the NMMO hydrates produce homogeneous solutions. Particularly at the heating rate 10℃ min^{-1} in Figure 3b these newly-observed melting peaks at 90℃ are on the extrapolated line of the (T_m)s of NMMO monohydrate, 80℃. Aforementioned, a transition from NMMO monohydrate to anhydrous NMMO takes place continuously with decreasing the value of n when the NMMO hydrates with $n<1$ are prepared by condensation. From this result, the existence of the crystal of C_4 is clearly verified because a solid–solid transition from C_1 to C_2 occurs at 90℃. In the case of anhydrous NMMO the crystal of only C_2 exists. Consequently the melting peaks are observed at 103 and 180℃.

Phase Behavior of Cellulose Solutions in NMMO Hydrates

Chanzy *et al.*[8] reported that the 10 wt% cellulose solutions in anhydrous NMMO and NMMO monohydrate crystallize at 100 and 20℃, respectively. It is recognized that cellulose molecules do not readily crystallize because of strong interactions with NMMO hydrate. To make out the phase behavior of the solutions in the NMMO hydrates, the crystallization mechanism of NMMO hydrate itself should be understood first. Figure 4 shows variation of the T_c of the NMMO hydrates with the cooling rate. The T_c was determined as follows. Firstly, the baseline of the thermogram was determined at the temperature from which the NMMO hydrate just began to melt. To guarantee being fully melted the specimen was heated up to the temperature equivalent to the baseline of the thermogram and loaded at the temperature for 30 s. From the recrystallization experiment, the crystallization peaks corresponding to various melting peaks could be analyzed.

As previously showed in Figure 3, the T_m is increased with increased the heating rate from 5 to 10℃ min^{-1}. It

is also expected that an increase of the cooling rate decreases the T_c of the NMMO hydrate component. If the scan rate is increased from 2 to 10℃ min^{-1} the crystallization peak shifts to the lower temperature. The T_m of NMMO monohydrate is little affected by the scan rate (see Figure 3, at $n=1.0$). However, the T_c is lowered by 10℃ with increasing the scan rate. The T_m of the NMMO monohydrate component remains constant irrespective of the cooling rate in the case of the NMMO hydrates with $n<1.0$. On the other hand, compared with the NMMO monohydrate and the NMMO hydrate with $n<1.0$ shows change in the crystallization temperature less than 5℃, which is slightly increased with increasing the scan rate. This result implies that the solution system gets more heterogeneous at lower hydration level if $n<1.0$.

It is worth noting that the NMMO monohydrate with $n=1.0$ gives one melting peak and one crystallization peaks. The cooling experiments on the NMMO hydrates with $n\leq0.83$ reveal that the first crystallization temperature after melting of C_1 crystal is observed in the range from 30 to 35℃. However, the secondary crystallization temperature after melting of C_2 and C_4 crystals increases with decreasing the hydration level; from 76 to 78℃ for $n=0.83$, from 76 to 80℃ for $n=0.65$, and from 76 to 80℃ for $n=0.45$. In addition, the secondary (76℃) and the third crystallization temperature (98℃) for $n=0.65$ at the scan rate 10℃ min^{-1} get very close each other at the scan rate 2℃ min^{-1}. Both (T_c)s shift and converge each other. The NMMO hydrates with very low hydration level such as $n=0.45$ show third crystallization temperature was rapidly decreased with decreasing the cooling rate. Three (T_c)s are observed; the first T_c is due to C_1, the second T_c is due to C_4, and the third is T_c due to C_2.

According to the phase diagram of NMMO hydrates with the hydration level reported by Chanzy *et al.*,[10] the melting peak at 94℃ ascribed to the solid–solid transition has little effect on the melting behavior. However, referring to the phase diagram obtained by recrystallization shown in Figure 5, a strong crystallization peak at 80℃ is observed for all the NMMO hydrates with $n<1$ irrespective of the cooling rate. For n, range from 0.83 to 0.9 the first T_c is a little increased with increasing the scan rate. Like the melting behavior this results from the instability of the mixed crystals of the NMMO hydrates. The instability is more pronounced at the higher cooling rate over the hydration level range. The crystals on the cooling phase diagram are denoted by S_1, S_2, and S_4 to differentiate them from the melting behavior of the crystals. The symbols, S_1, S_2, and S_4, in Figure 5 correspond to those, C_1, C_2, and C_4, in Figure 3, respectively. From the solid–solid transition from NMMO monohydrate to anhydrous NMMO on this cooling phase diagram we could observe the S_4 region, which has never been reported by others.

Figure 6 shows DSC thermogram of the cellulose solutions in NMMO hydrate with $n=0.65$. The T_m of the hydrate component in the solution is observed at lower temperature than the T_m of NMMO monohydrate (78℃). As given in Table II, the T_m is lowered as the concentration of cellulose is increased from 6 to 20 wt%. This seems to result from the stronger interactions between

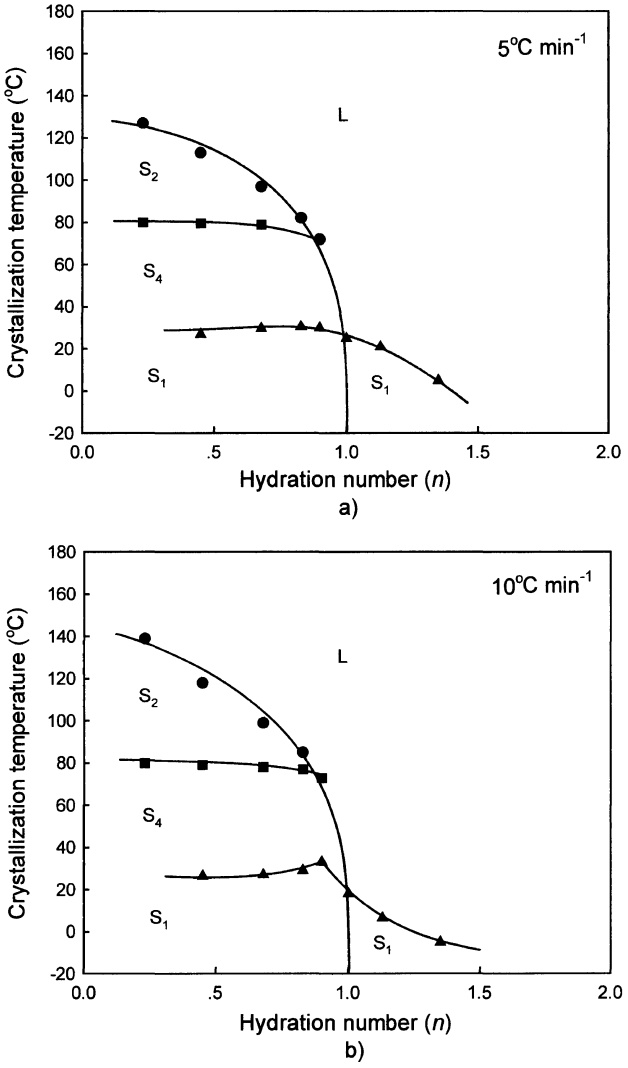

Figure 5. Relationship between crystallization temperature and hydration number in the NMMO hydrates system: a) 5℃ min^{-1} and b) 10℃ min^{-1}.

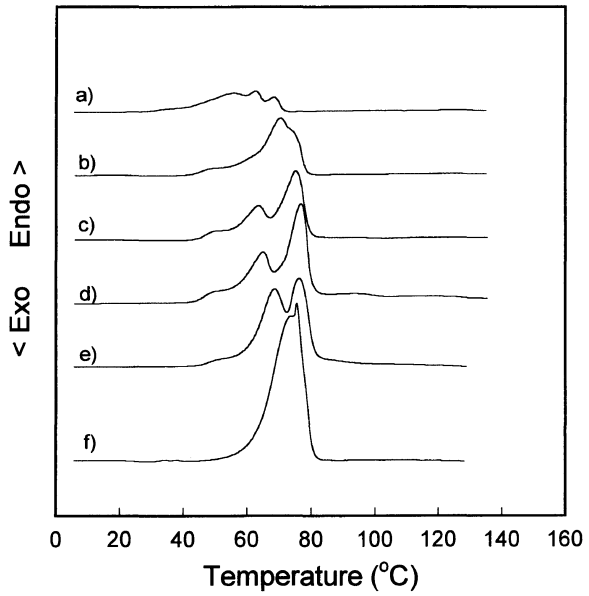

Figure 6. DSC thermograms of cellulose (DP_w 600) solution in NMMO hydrate ($n=0.65$) at the heating rate 5℃ min^{-1}, showing the effect of cellulose concentration; a) 20 wt%, b) 18 wt%, c) 15 wt%, d) 12 wt%, e) 10 wt%, and f) 6 wt%.

Table II. Variation of melting point ($T_{m,l}$, $T_{m,h}$) and shoulder temperature (T_s) of cellulose (DP_w 600) solution in NMMO hydrate (n=0.65)

Con./wt%	Melting temp.		Shoulder temp.
	$T_{m,l}$/℃	$T_{m,h}$/℃	T_s/℃
6	72.71	76.06	—
10	67.64	76.49	50.12
12	63.64	76.21	48.91
15	62.28	75.22	49.10
18	—	(74.34)	48.25
20	62.78	68.79	55.83

$T_{m,l}$: lower melting peak. $T_{m,h}$: higher melting peak.
T_s: weak shoulder peak.

Table III. Variation of melting and crystallization temperature of cellulose (DP_w 600) solution in NMMO hydrate (n=0.65)

Con./wt%		scan rate/℃min^{-1}	
		2	5
6	$T_{m,l}$	71	72.7
	$T_{m,h}$	74.7	76
	T_c	6—12	—
10	$T_{m,l}$	66.6	67.6
	$T_{m,h}$	75.1	76.5
	T_c	—	—

$T_{m,l}$: lower melting peak. $T_{m,h}$: higher melting peak.
T_c: crystallization peak.

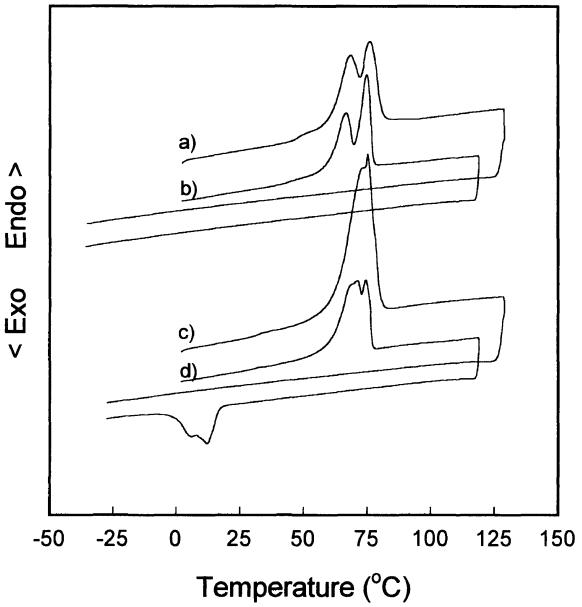

Figure 7. DSC thermograms of cellulose (DP_w 600) solution in NMMO hydrate (n=0.65) at the heating rate of 5℃ min^{-1} (a), c)) and 2℃ min^{-1} (b), d)), showing the effect of cellulose concentration; a), b) 10 wt% and c), d) 6 wt%.

NMMO hydrate and cellulose molecules at higher cellulose concentration.[10]

Chanzy *et al.*[10] ascribed the broad peak in the vicinity of 60℃ to recrystallization in the DSC characterization of low molecular weight cellulose (DP_w 120) solution in NMMO monohydrate. Such a T_m depression is obliged to the small crystallite size,[26] which phenomenon is also well documented in semicrystalline polymers.[27] To our judgement, the peak separation in the vicinity of 60℃ with increasing concentration reflects the increase of the interaction between cellulose and NMMO hydrate through hydrogen bonding between the hydroxyl groups on the cellulose and the N–O group on the NMMO is increased. Consequently, the solution deviates from the ideal solution (c=0.5) with increasing cellulose concentration.

The interaction during melting of the cellulose solutions in NMMO hydrates can be also verified by the crystallization experiments. Figure 7 shows the melting and crystallization behaviors of the cellulose solutions in NMMO hydrate with n=0.65. At the cellulose concentration 10 wt% the crystallization behavior is not observed but at 6 wt% the crystallization peak is observed in the range from 6 to 12℃ at the scan rate 2℃ min^{-1}. The pure NMMO hydrate with n=0.65 exhibits the first crystallization at 25℃ (see Figure 4).

Referring to Table III, this indicates that the first T_c of the NMMO hydrate in the 6 wt% cellulose solution becomes lowered by the range from 13 to 19℃, which stands for the dominance of solvent characteristics resulting from weaker interaction between NMMO hydrate and cellulose at lower cellulose concentration.[28] The T_c of the NMMO hydrate in the dilute cellulose solution (say, lower than 6 wt%) is not change to low temperature with further dilution while the NMMO hydrate in the cellulose solution. This indicates that the solvent crystallizes first in the dilute solution.

The 10 wt% cellulose (DP_w 1500) solution in the NMMO monohydrate crystallizes at 20℃, which was measured by cooling the cellulose solution to room temperature in the preheated glass slide on the optical microscope.[8] In this study the concentration and temperature for crystallization are measured to be 6 wt% and the range from 6 to 12℃ (at the cooling rate 2℃ min^{-1}), respectively. These values are lower than the previously reported because we used different cellulose with lower molecular weight (DP_w 600) and NMMO hydrate with n =0.65.

The cellulose solutions in NMMO monohydrate produces spherulites with proceeding crystallization, whose size is decreased as the concentration is increased.[8] The cellulose solutions in anhydrous NMMO crystallize at 100℃, producing a cellulated structure.[8] Chanzy *et al.*[9] and Navard and Haudin[15] observed a phase transition from anisotropic to isotropic takes place at the range from 88 to 90℃ from the rheological measurement of cellulose (DP_w 900) solutions in NMMO hydrates with n, range from 0.3 to 0.54, which hydrates were prepared by simple mixing of anhydrous NMMO and water. Referring to our result for NMMO hydrates with n, range from 0.45 to 0.65 the secondary and the third crystallization takes place in the range from 80 to 120℃. Particularly at n=0.65 crystallization occurs in the range from 80 to 100℃. This discrepancy suggests that the mesophase characteristics observed by above authors resulted from the unmelted crystals of anhydrous NMMO rather than from ordering of cellulose molecules. In fact, we found that the anisotropic-isotropic phase transition took place in the range from 105 to 127.5℃ when the cellulose solution was prepared by using a fully melted NMMO hydrates.[17]

CONCLUSION

In the observation of the thermal properties of NMMO hydrates, a careful attention should be paid. In the case of NMMO hydrates the DSC measurement should guarantee no evaporation of water from the hydrates at the elevated temperature. The phase behavior of the cellulose solutions in NMMO hydrates should also be carefully investigated. These results have engineering significance in the design of lyocell fiber spinning processes. It further suggests that the phase of spinning dope solution might be different even at the same composition and temperature depending on the preparative methods of the solution, in which case different spinning conditions should be adopted.

REFERENCES

1. G. Graenacher and R. Sallmann, U. S. Patent, 2 179 181 (Nov. 7, 1939).
2. D. L. Johnson, U. S. Patent, 3 447 939 (Jun. 3, 1969).
3. D. L. Johnson, U. S. Patent, 3 508 941 (Apr. 28, 1970).
4. C. C. McCorsley and J. K. Varga, U. S. Patent, 4 142 913 (Mar. 6, 1979).
5. N. E. Franks and S. K. Varga, U. S. Patent, 4 145 532 (Mar. 20, 1979).
6. N. E. Franks and S. K. Varga, U. S. Patent, 4 196 282 (Apr. 1, 1980).
7. C. C. McCorsley, U. S. Patent, 4 246 221 (Jan. 20, 1981).
8. H. Chanzy, M. Dube, and R. H. Marchessault, *J. Polym. Sci., Polym. Lett. Ed.*, **17**, 219 (1978).
9. H. Chanzy, A. Peguy, S. Chaunis, and P. Monzie, *J. Polym. Sci., Polym. Phys. Ed.*, **18**, 1137 (1980).
10. H. Chanzy, S. Nawrot, A. Peguy, and P. Smith, *J. Polym. Sci., Polym. Phys. Ed.*, **20**, 1909 (1982).
11. E. Maia, A. Peguy, and S. Perez, *Acta Crystallogr., B: Struct. Sci.*, **37**, 1858 (1981).
12. E. Maia and S. Perez, *Acta Crystallogr., B: Struct. Sci.*, **38**, 849 (1982).
13. D. Gagnaire, D. Mancier, and M. Vincendon, *J. Polym. Sci., Polym. Chem. Ed.*, **18**, 1137 (1980).
14. D. L. Patel and R. D. Gilbert, *J. Polym. Sci., Polym. Phys. Ed.*, **19**, 1231 (1981).
15. P. Navard and J. M. Haudin, *Br. Polym. J.*, **22**, 174 (1980).
16. B. C. Kim, W. S. Lee, S. M. Jo, C. S. Park, D. B. Kim, and Y. M. Lee, *Polym. Mater. Sci. and Eng.*, **77**, 475 (1997).
17. D. B. Kim, W. S. Lee, and H. J. Kang, *Polymer (Korea)*, **22**, 770 (1998).
18. D. B. Kim, W. S. Lee, S. M. Jo, Y. M. Lee, and B. C. Kim, *Polym. J.*, **33**, 18 (2001).
19. D. Loubinoux and S. Chauis, *Text. Res. J.*, **57**, 61 (1987).
20. P. Navard and J. M. Haudin, *Polym. Pro. Eng.*, **3**, 291 (1985).
21. H. Chanzy, M. Paillet, and R. Hagege, *Polymer*, **31**, 400 (1990).
22. S. W. Chun, S. M. Jo, W. S. Lee, and J. D. Kim, *J. Kor. Fiber. Soc.*, **29**, 44 (1992).
23. D. B. Kim, W. S. Lee, B. C. Kim, S. M. Jo, J. S. Park, and Y. M. Lee, *Polymer (Korea)*, **22**, 231 (1998).
24. K. Fischer, *Angew. Chem.*, **48**, 394 (1935).
25. H. Chanzy, *Carbohydrate Polymers*, **2**, 229 (1982).
26. E. A. Turi, "Thermal Characterization of Polymeric Materials", Academic Press, Inc., New York, N.Y., 1997, vol. 1, p 415.
27. B. Wunderlich, "Macromolecular Physics", Academic Press, Inc., New York, N.Y., 1976, vol. 2, p 348.
28. S. H. Park, Y. H. Jeong, W. S. Lee, and H. J. Kang, *Polymer (Korea)*, **22**, 779 (1998).